Fig. 1 IgE amino acid surface exposure using the Padlan and Davies 1986 model.

Residue	Surface Area	average/5	>50	>80	
ARG_1	270.322723				
ASP_2	139.374542				
PHE_3	64.298927	117.361489	1	1	
THR_4	46.170193	64.494911	1	0	
PRO_5	66.64106	39.0209532	0	0	
PRO_6	5.989833	29.3644934	0	0	
THR_7	12.004753	21.4426604	0	0	
VAL_8	16.016628	8.6200336	0	0	
LYS_9	6.561028	10.2708042	0	0	
ILE_10	2.527926	9.5044914	0	0	
LEU_11	14.243686	13.375776	0	0	
GLN_12	8.173189	19.2992118	0	0	
SER_13	35.373051	29.1890154	0	0	
SER_14	36.178207	32.6313328	0	0	
CYS_15	51.976944	39.0100884	0	0	
ASP_16	31.455273	45.6135238	0	0	
GLY_17	40.066967	50.0871888	1	0	
GLY_18	68.390228	46.9957994	0	0	
GLY_19	58.546532	59.6253914	1	0	P5
HIS_20	36.519997	63.4215874	1	0	P5
PHE_21	94.603233	68.1998406	1	0	P5
PRO_22	59.047947	65.8523506	1	0	P5
PRO_23	92.281494	62.0824146	1	0	P5
THR_24	46.809082	50.1635586	1	0	P5
ILE_25	17.670317	38.6392736	0	0	
GLN_26	35.008953	21.6261078	0	0	
LEU_27	1.426522	12.5259452	0	0	
LEU_28	7.215665	10.5518628	0	0	
CYS_29	1.308269	3.5500722	0	0	
LEU_30	7.799905	4.8164434	0	0	
VAL_31	0	4.0672202	0	0	
SER_32	7.758378	3.8055664	0	0	
GLY_33	3.469549	9.5755666	0	0	
TYR_34	0	20.7786542	0	0	
THR_35	36.649906	28.9967052	0	0	
PRO_36	56.015438	50.2230378	1	0	P6
GLY_37	48.848633	57.590085	1	0	P6
THR_38	109.601212	73.50021	1	0	P6
ILE_39	36.835236	70.1846368	1	0	P6
ASN_40	116.200531	73.2560022	1	0	P6
ILE_41	39.437572	51.7217026	1	0	P6
THR_42	64.20546	49.2710734	0	0	
TRP_43	1.929714	35.2314448	0	0	
LEU_44	24.58209	49.7665942	0	0	
GLU_45	46.002388	50.9119188	1	0	
ASP_46	112.113319	74.3084848	1	0	
GLY_47	69.932083	91.0816862	1	1	
GLN_48	118.912544	85.9516244	1	1	P1
VAL_49	108.448097	91.6210626	1	1	

MET_50	20.352079	89.4386316	1	1
ASP_51	140.46051	77.095856	1	0
VAL_52	59.019928	65.664336	1	0
ASP_53	57.198666	72.8180802	1	0
LEU_54	51.290497	45.9930286	0	0
SER_55	56.1208	49.3437382	0	0
THR_56	6.335252	47.723164	0	0
ALA_57	75.773476	43.8934994	0	0
SER_58	49.095795	51.656078	1	0
THR_59	32.142174	59.4056414	1	0
THR_60	94.933693	72.6291262	1	0
GLN_61	45.083069	73.3905916	1	0 P2
GLU_62	141.8909	99.7907822	1	1
GLY_63	52.903122	90.626043	1	1
GLU_64	164.143127	83.4067496	1	1
LEU_65	49.109997	57.2201384	1	1
ALA_66	8.986602	47.5504318	0	0
SER_67	10.957844	17.0083172	0	0
THR_68	4.554589	7.3021006	0	0
GLN_69	11.432554	7.2534874	0	0
SER_70	0.578914	5.0619186	0	0
GLU_71	8.743536	8.9567614	0	0
LEU_72	0	10.8120506	0	0
THR_73	24.028803	23.2812776	0	0
LEU_74	20.709	37.264713	0	0
SER_75	62.925049	69.375269	1	0
GLN_76	78.660713	79.6644746	1	0
LYS_77	160.55278	78.1594206	1	0
HIS_78	75.474831	77.9196576	1	0
TRP_79	13.18373	76.6092892	1	0 P3
LEU_80	61.726234	70.354977	1	0
SER_81	72.108871	73.244224	1	0
ASP_82	129.281219	81.9731098	1	1
ARG_83	89.921066	69.9061278	1	0
THR_84	56.828159	58.6259284	1	0
TYR_85	1.391324	32.7696846	0	0
THR_86	15.707874	23.8688072	0	0
CYS_87	0	12.5031754	0	0
GLN_88	45.416679	24.6922706	0	0
VAL_89	0	22.314276	0	0
THR_90	62.3368	48.4045714	0	0
TYR_91	3.817901	45.5941352	0	0
GLN_92	130.451477	47.9061642	0	0
GLY_93	31.364498	62.7324992	1	0
HIS_94	11.560145	91.805003	1	1
THR_95	136.468475	85.5324108	1	1
PHE_96	149.18042	87.190961	1	1
GLU_97	99.088516	90.6138422	1	1
ASP_98	39.657249	75.8683994	1	1
SER_99	28.674551	62.1985202	1	0
THR_100	62.741261	62.538042	1	0
LYS_101	80.831024	61.892236	1	0
LYS_102	100.786125	65.3434144	1	0 P4
CYS_103	36.428219	66.2248162	1	0
ALA_104	45.930443	63.0386422	1	0
ASP 105	67.14827	64.611715	1	0

SER_106	64.9001548	71.4769134	1	0

Fig. 2 Scheme 1, solid phase peptide synthesis

Scheme 1

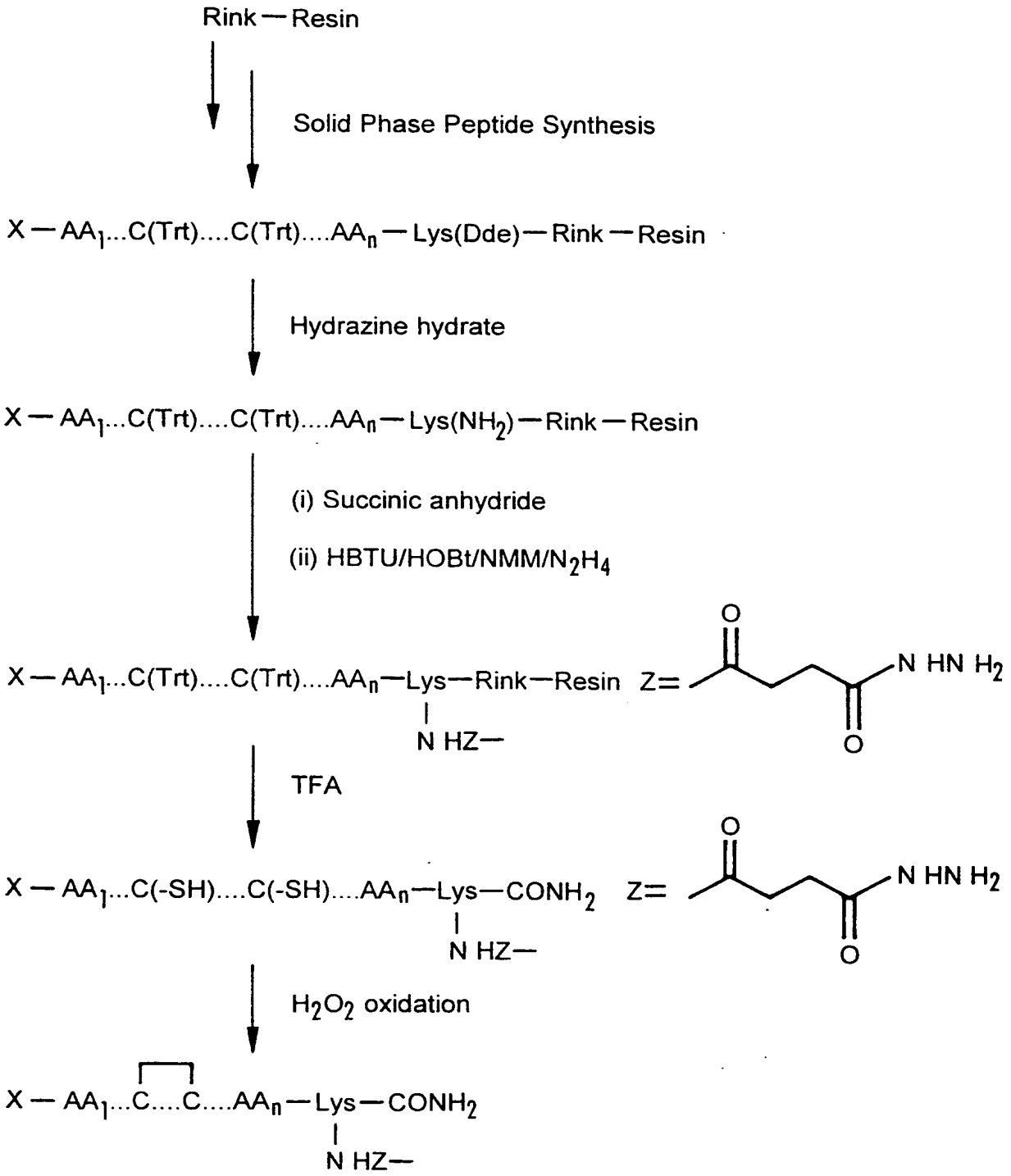

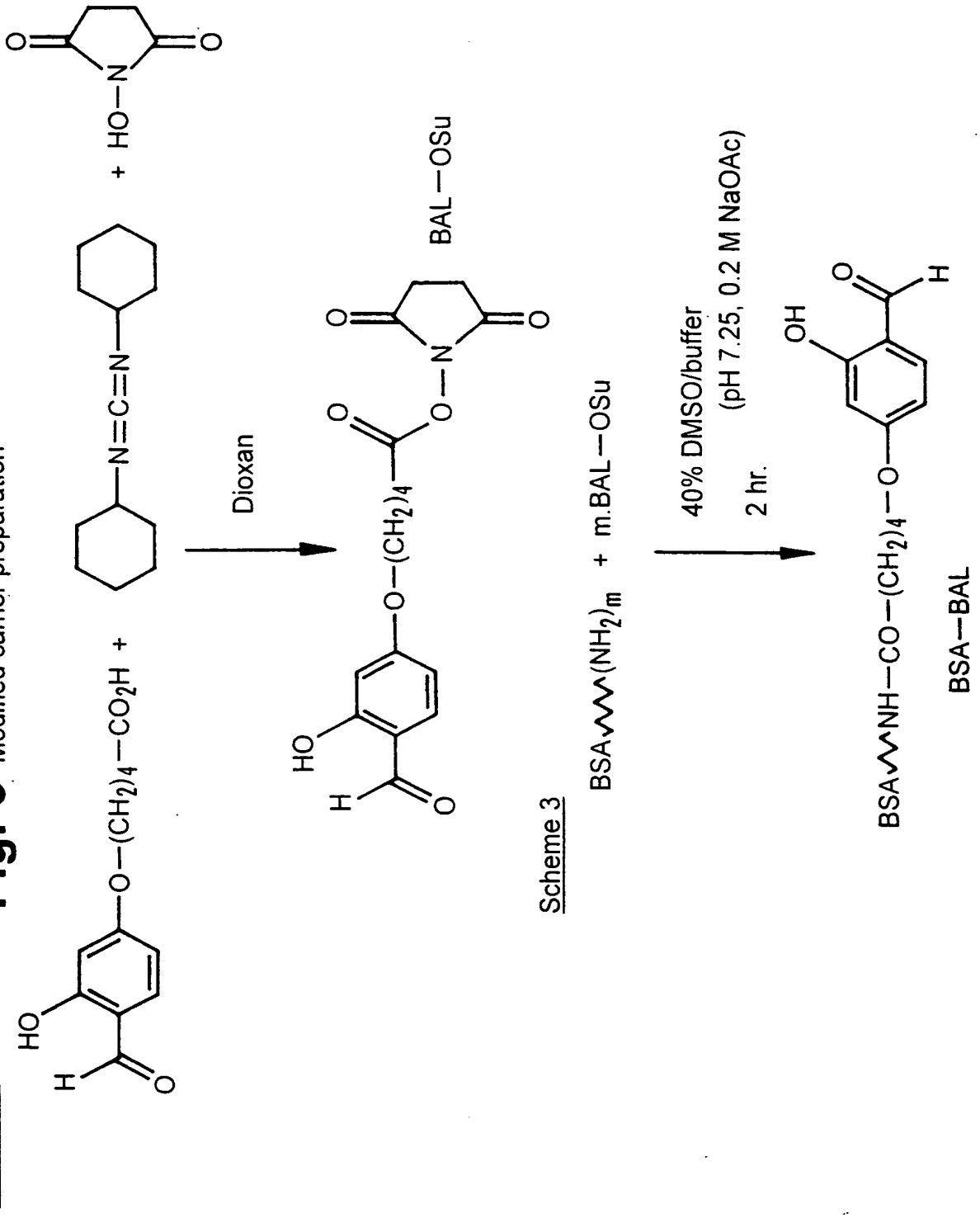

Fig. 3 Modified carrier preparation

Fig. 4 Chemistry Scheme 4, Peptide/carrier conjugation

Scheme 4

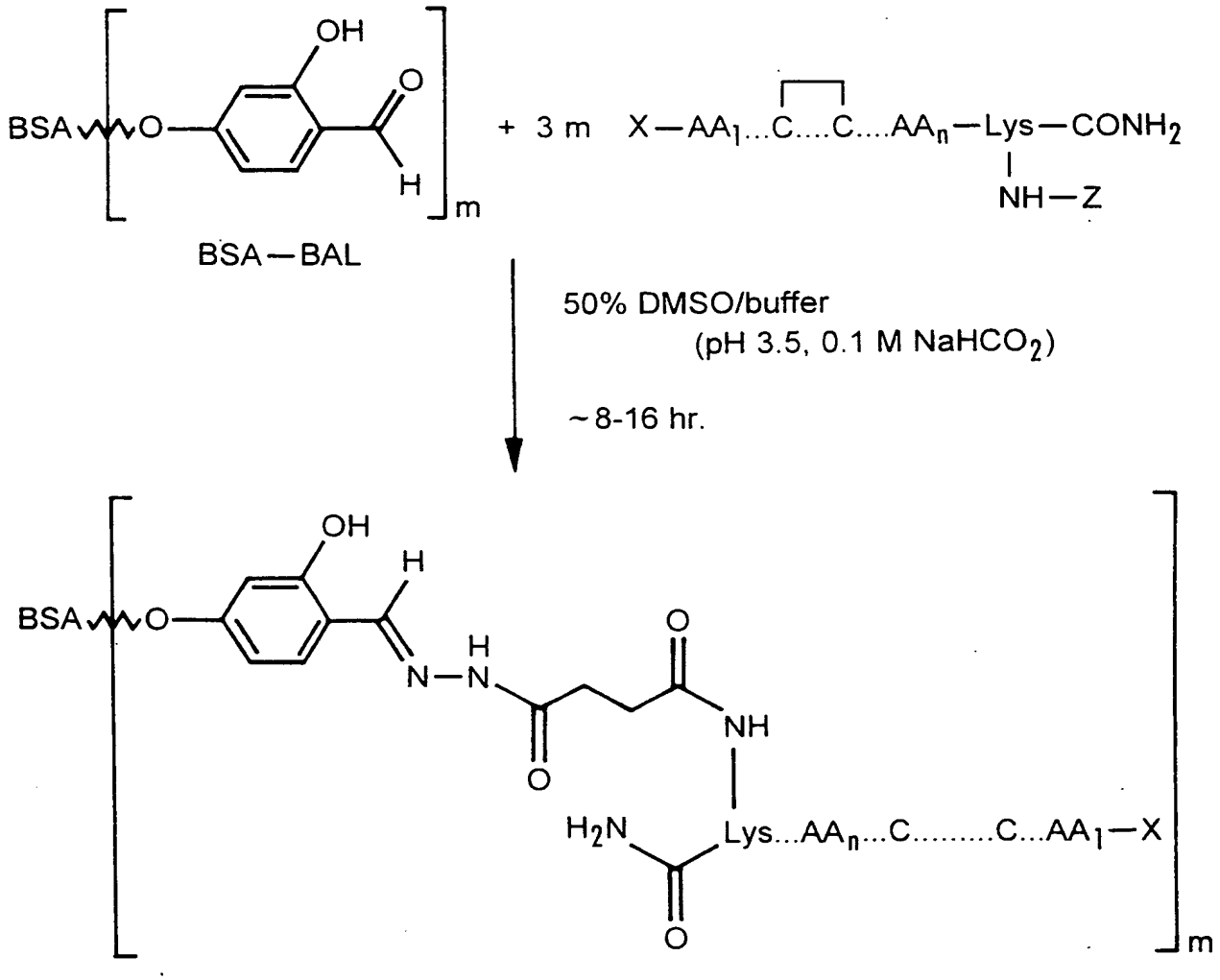

Fig. 5 C67-8 Anti-IgE Data

A.

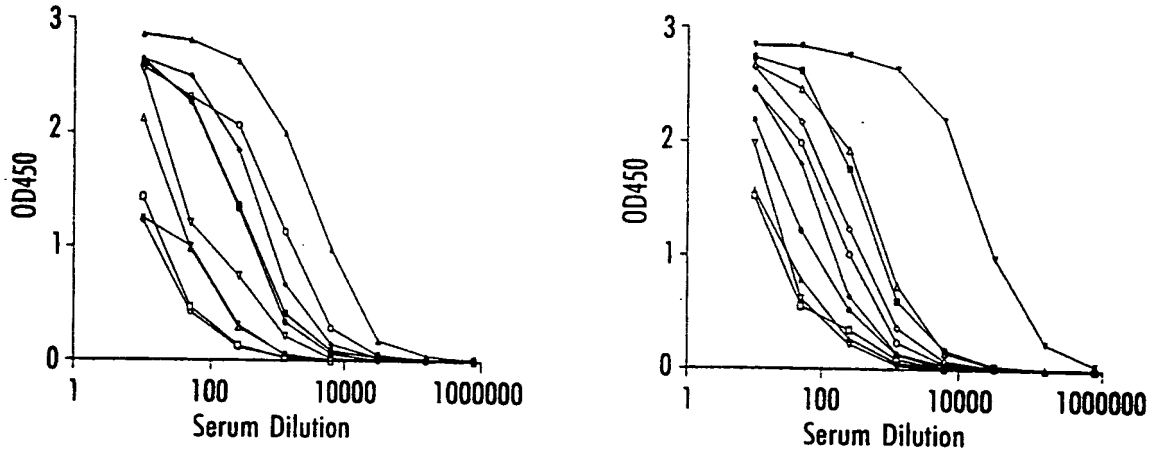

B.

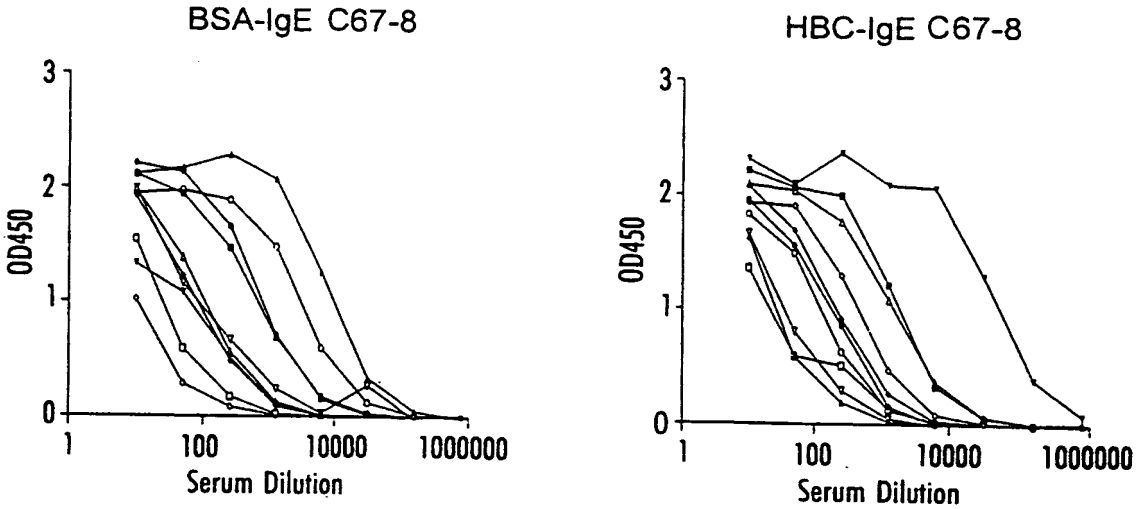

Fig. 6 Competition assay with soluble IgE and IgE C67-8 peptide.

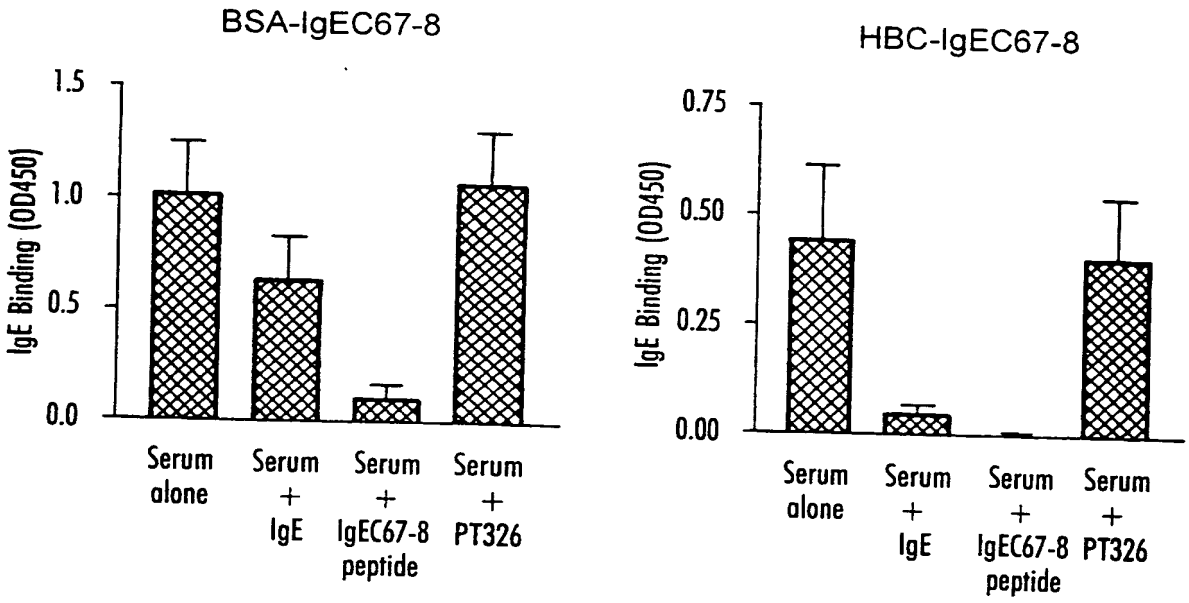

Fig. 7 PT1079 Anti-IgE Data

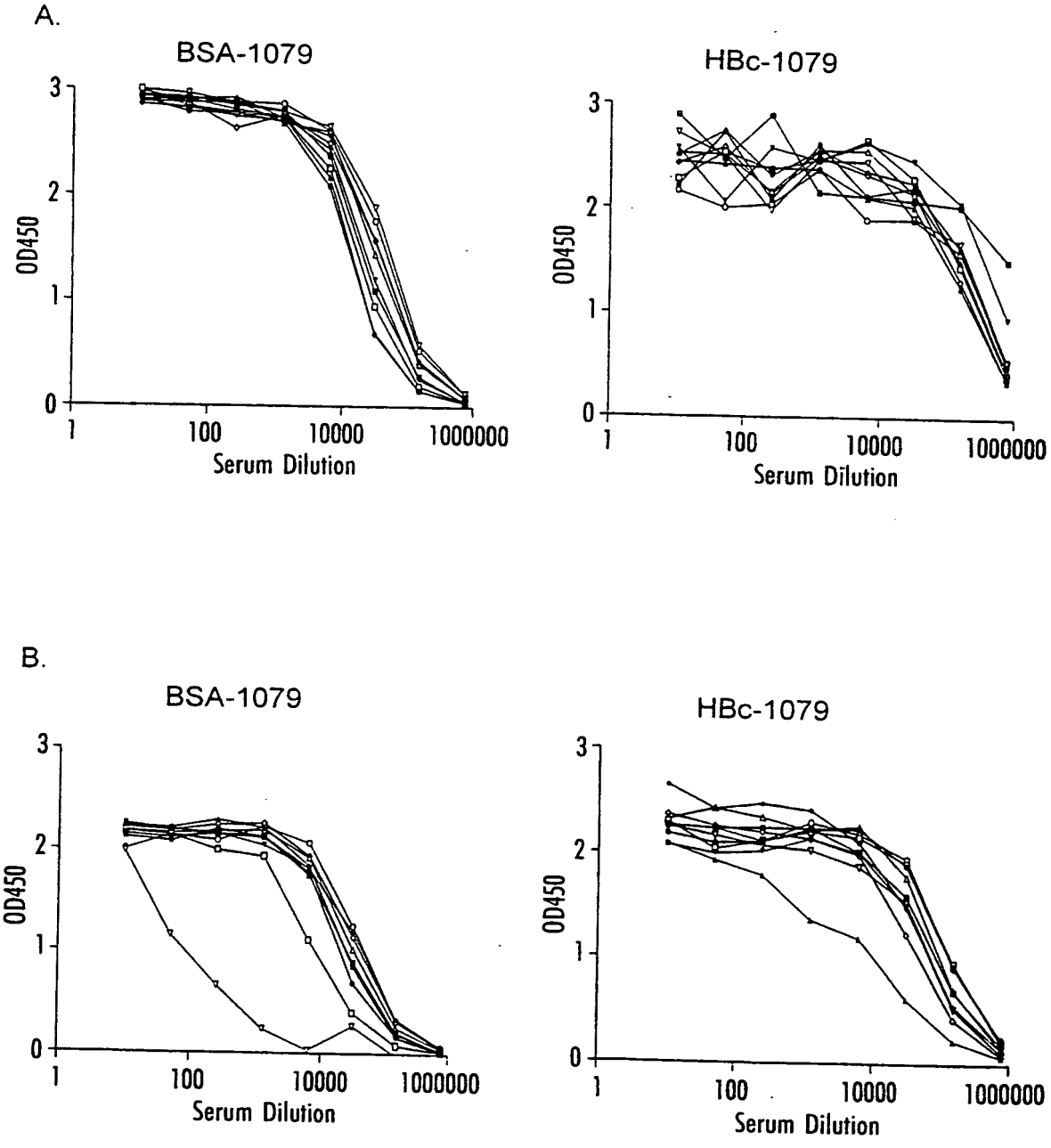

Fig. 8 Competition assay with soluble IgE and PT1079 peptide.

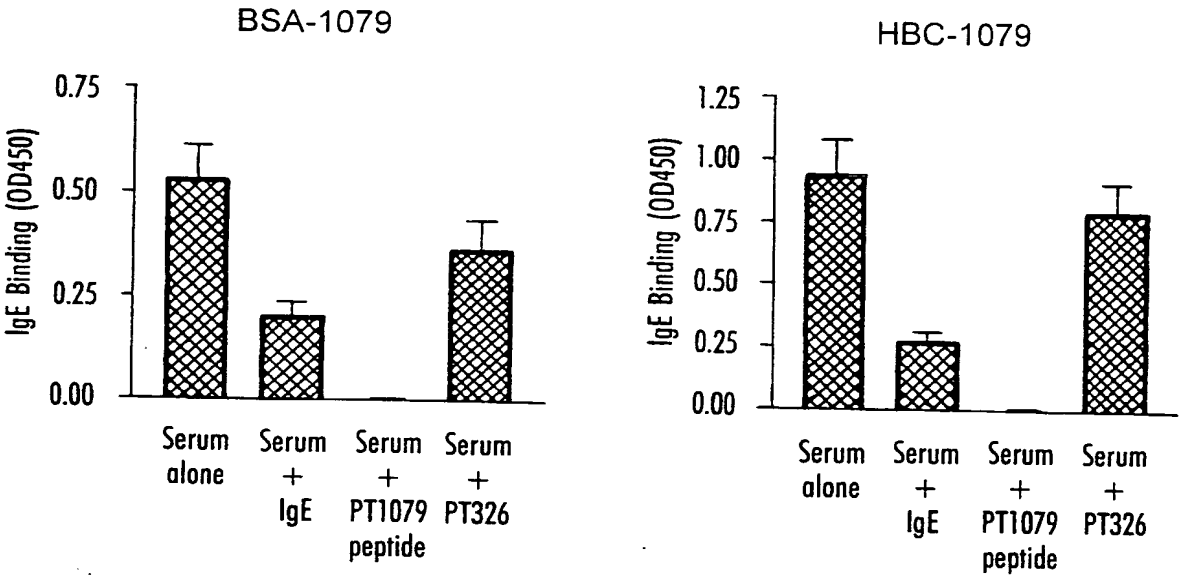

Fig. 9 PT1078 Anti-IgE Data

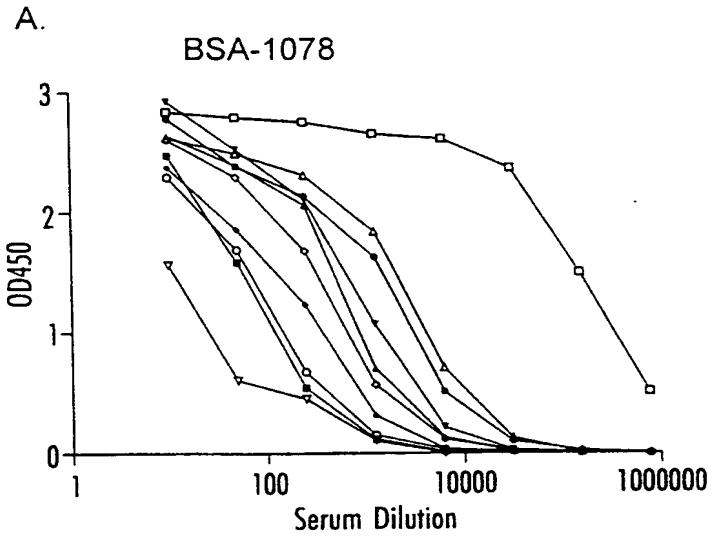

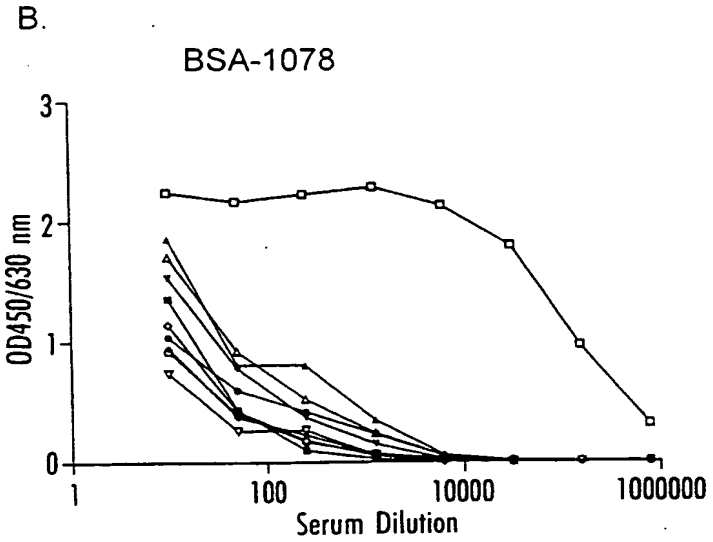

Fig. 10 Competition assay with soluble IgE and PT1078 peptide.

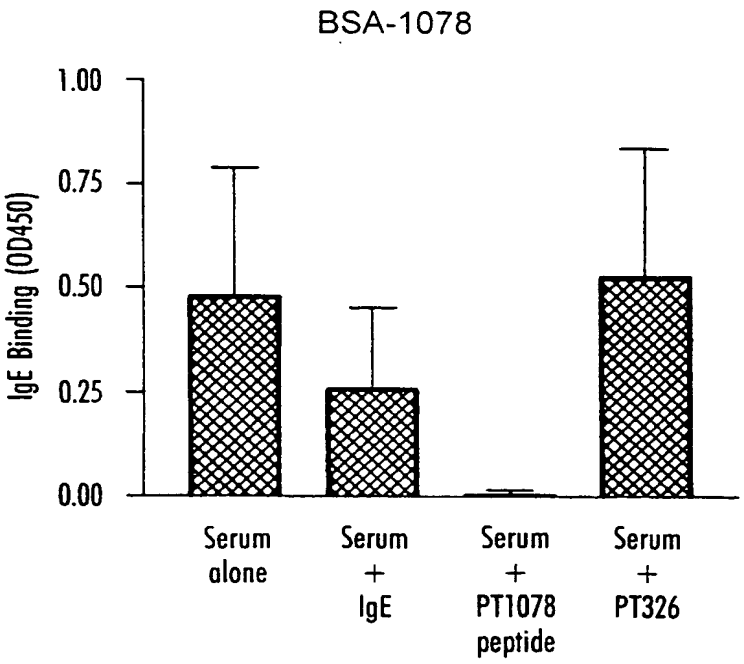

Fig. 11 PT1079gs Anti-IgE Data

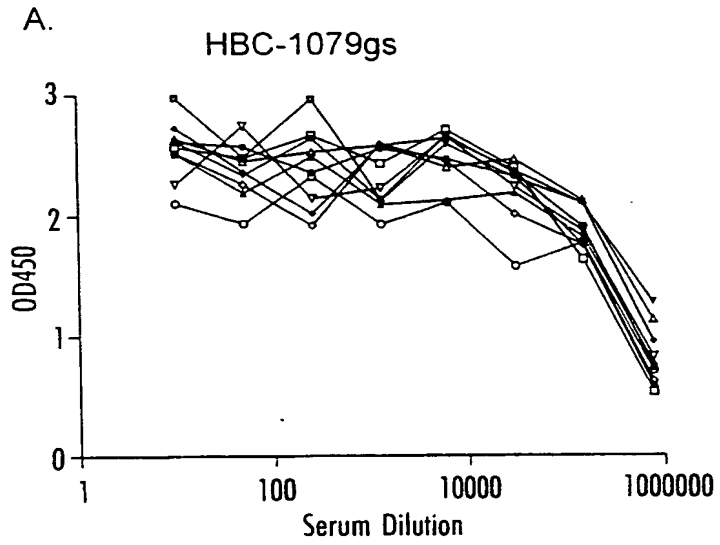

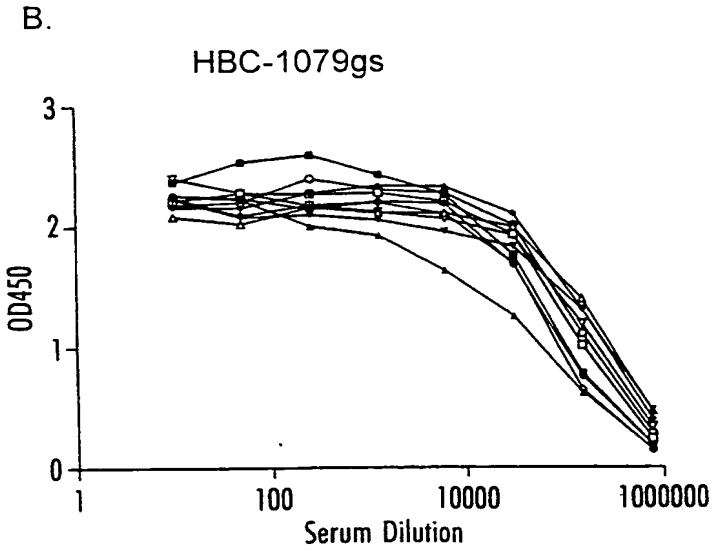

Fig. 12 Competition assay with soluble IgE and PT1079 peptide.

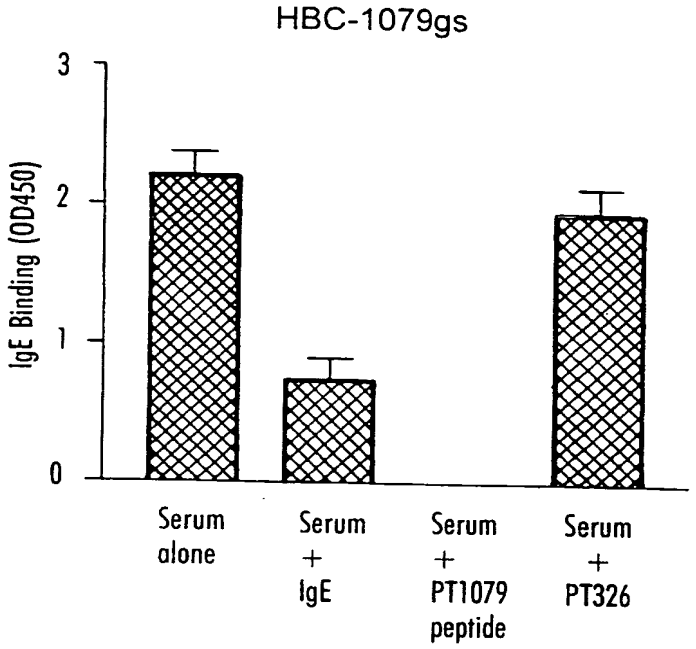

Fig. 13 Inhibitory Activity of Mouse BSA-C67-8 induced Antisera

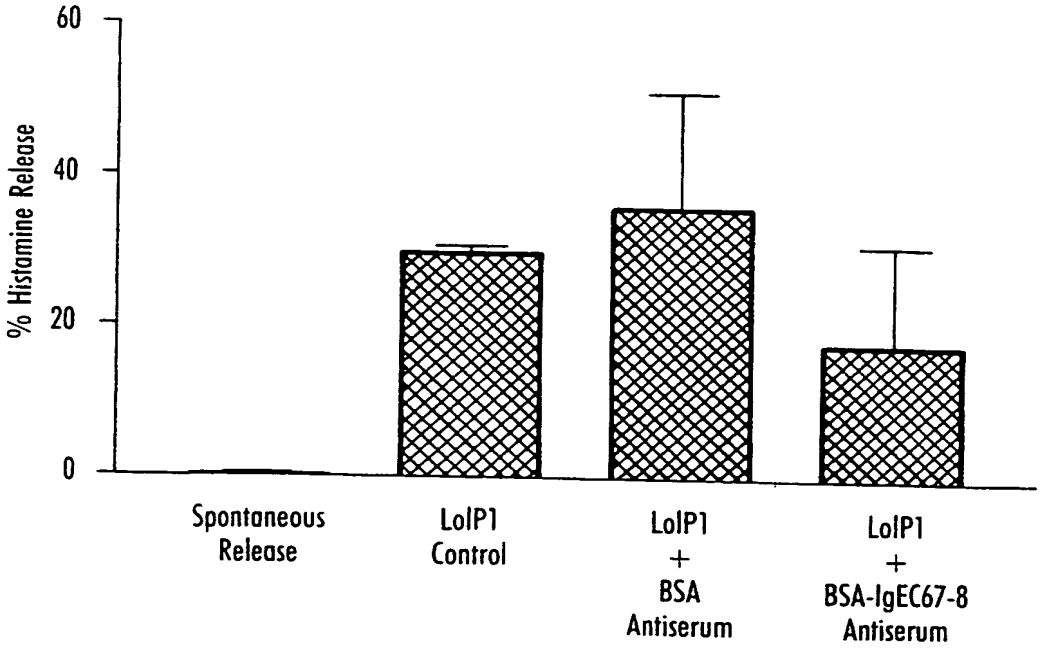

Fig. 14 Inhibitory Activity of Mouse Antisera induced by BSA-1078 and BSA-1079.

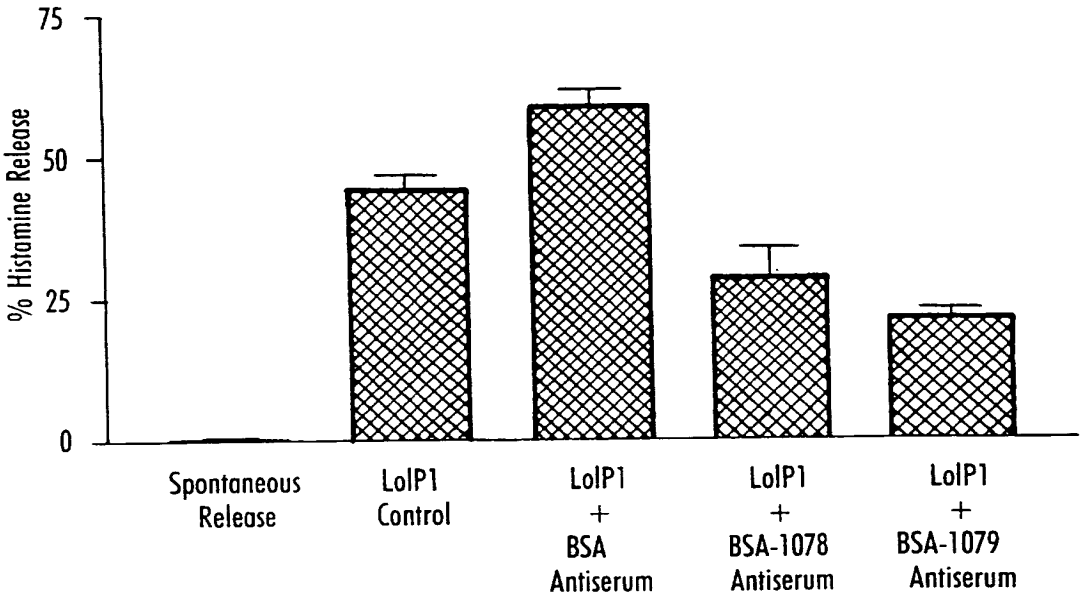

Fig.15 Inhibitory Activity of Mouse Antisera induced by HBC-C67-8, HBC-1078, HBC-1079 and HBC-1079gs

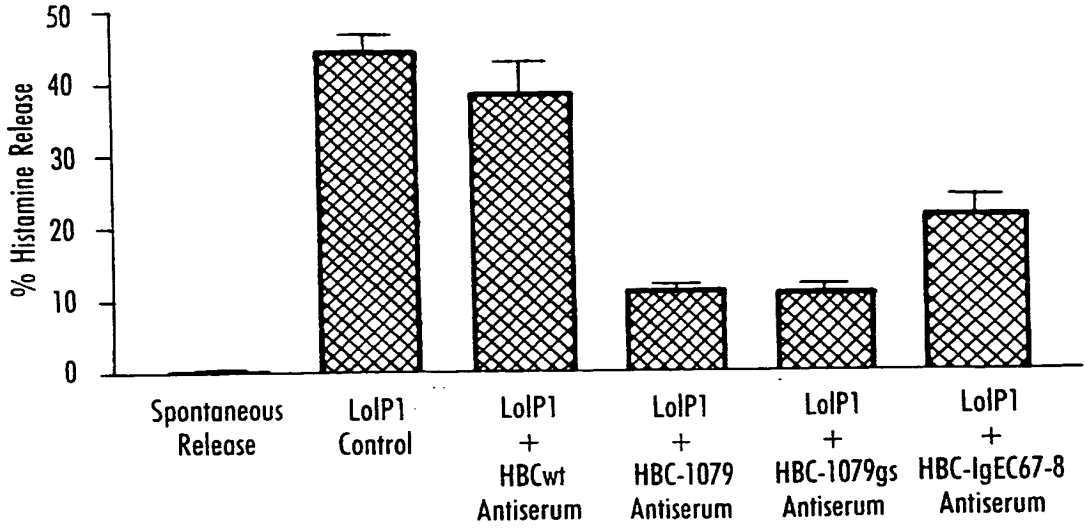

Fig. 16 shows the concentration dependent binding of antibody PTmAb0005 and PTmAb0011 to IgE.

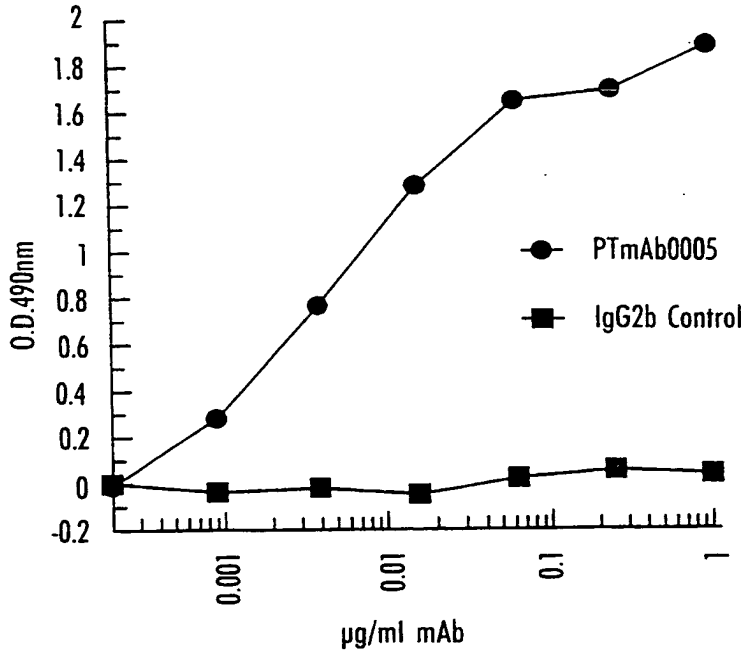

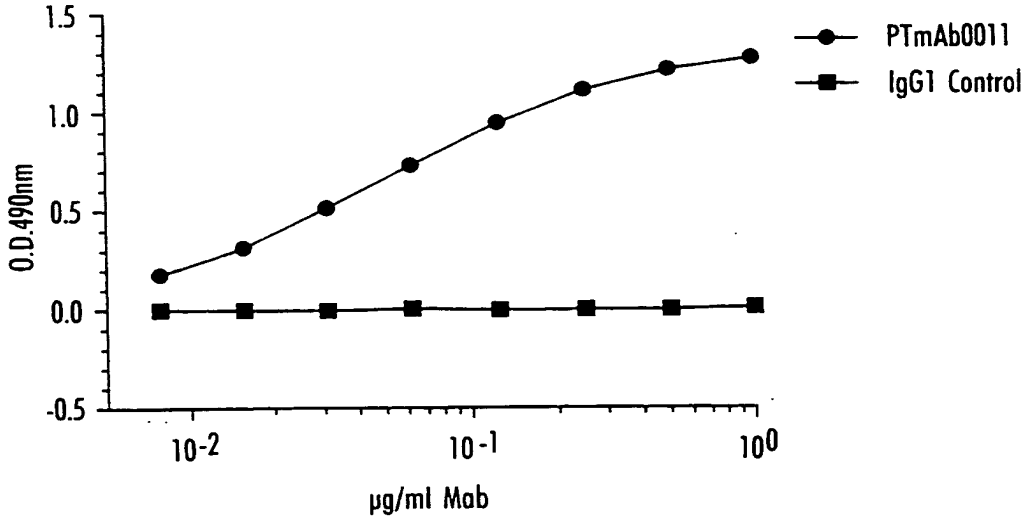

Fig. 17 shows the concentration dependent inhibition of IgE binding to an FcεR1α/IgG construct with antibody PTmAb0005 and PTmAb0011 compared to control.

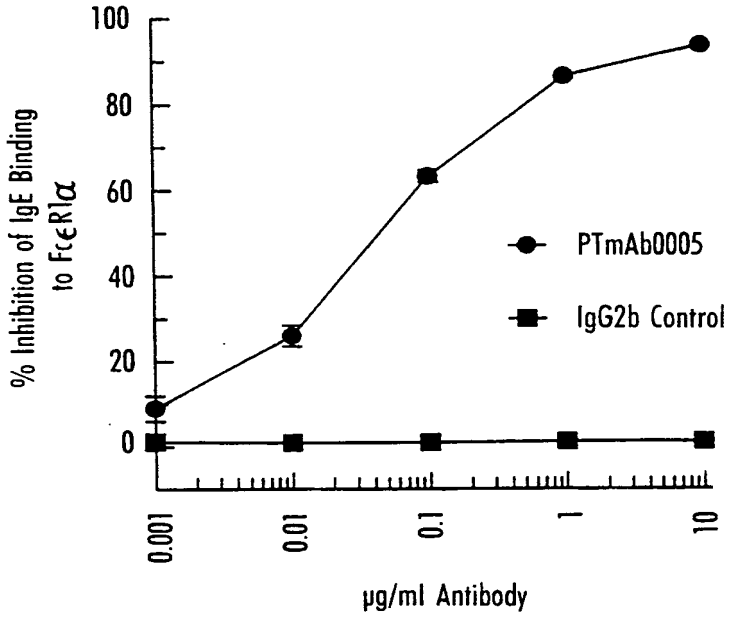

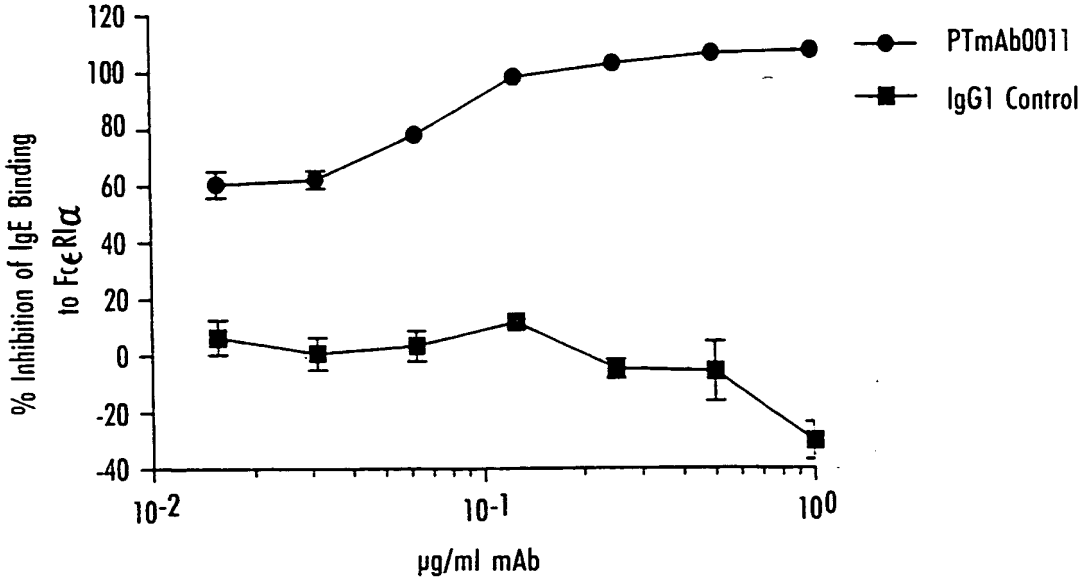

Fig. 18 shows the concentration dependent inhibition of IgE binding to clipped ectodomain of FcεRIα-bound directly to plastic plates, by antibody PTmAb0005, compared to control.

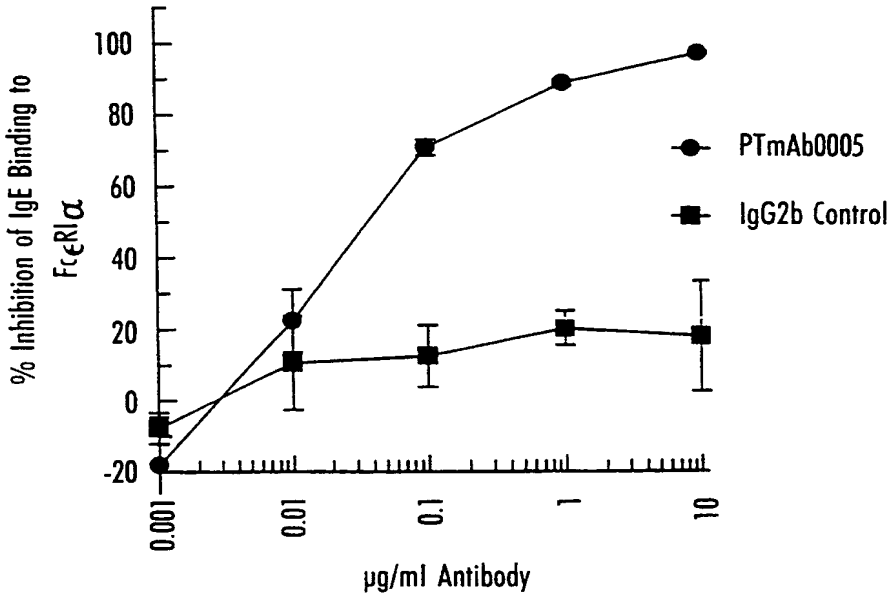

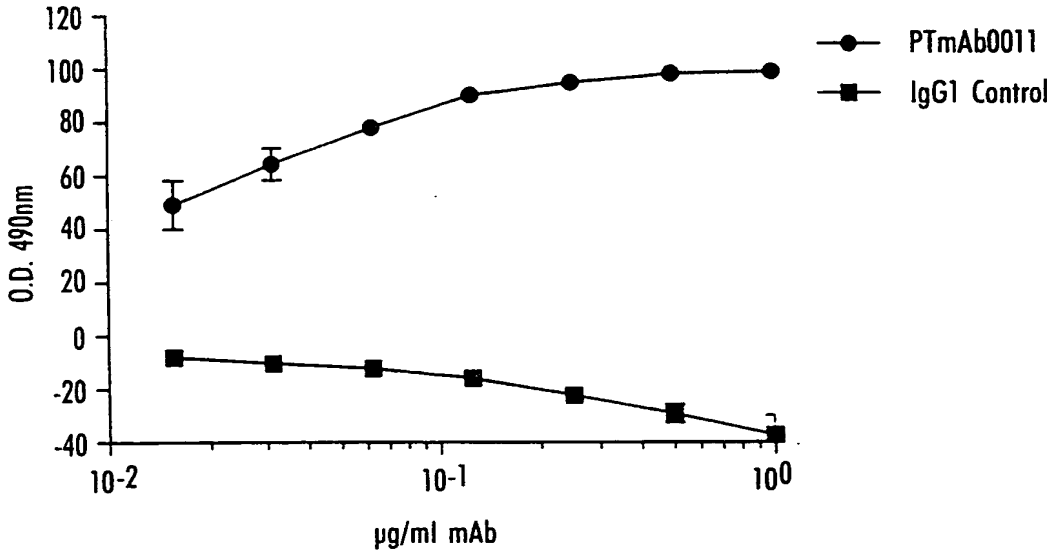

Fig. 19 shows IgE binding to FcεRII (CD23) by antibody PTmAb0005 (GE-1) and PTmAb0011.

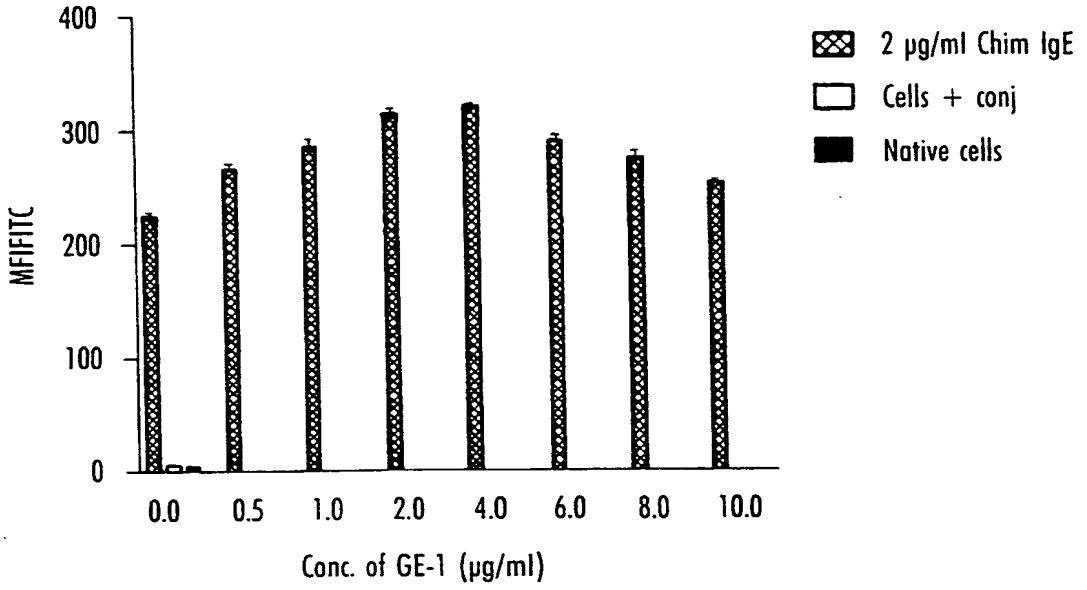

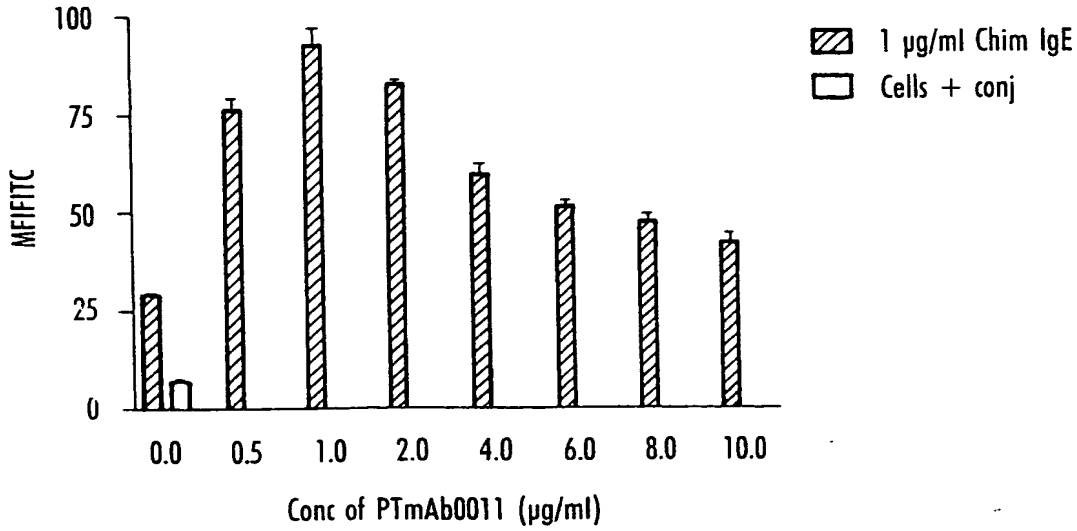

Fig. 20 shows the concentration-dependent blocking of histamine release from allergic human blood basophils with antibody PTmAb0005 and PTmAb0011 compared to control.

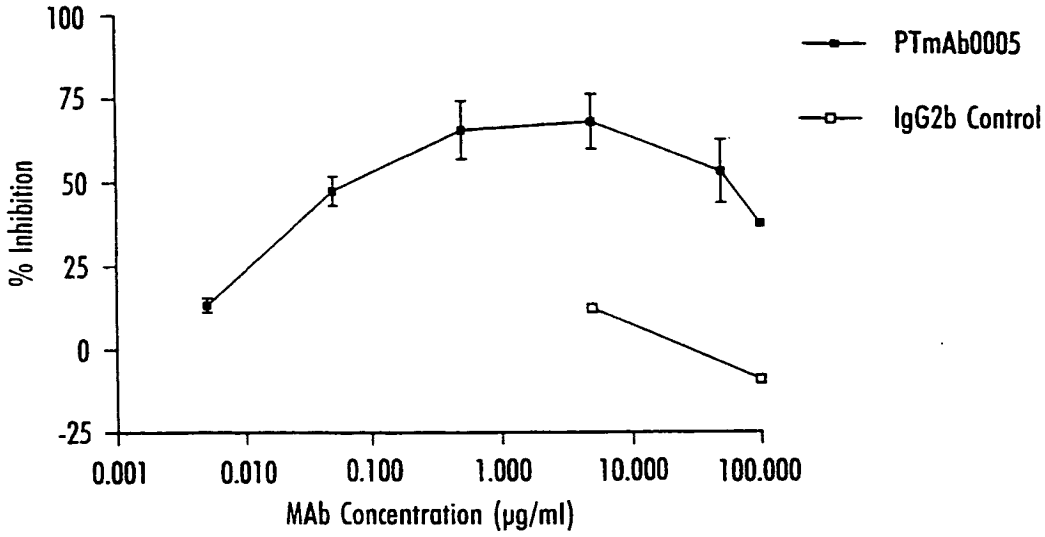

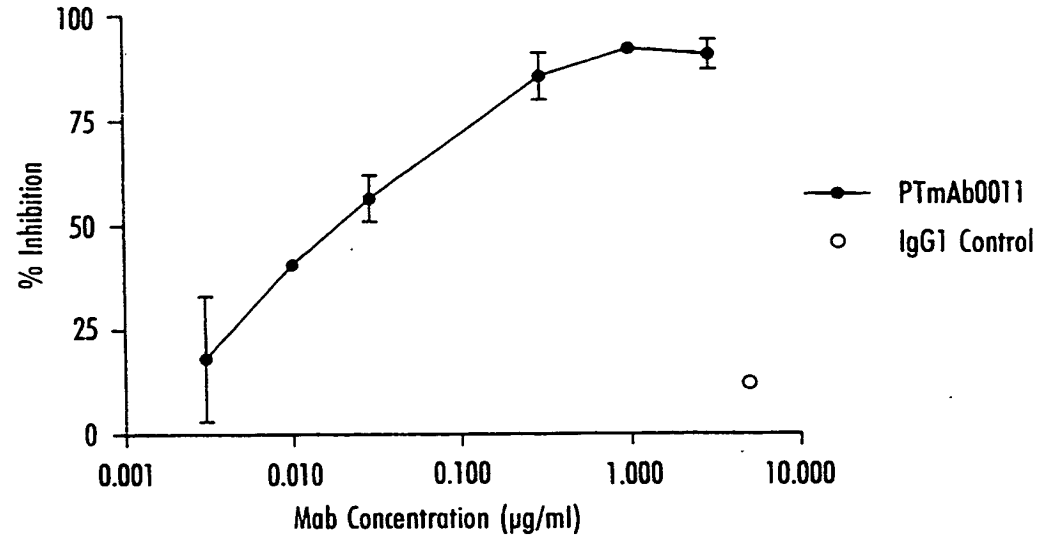

Fig. 21

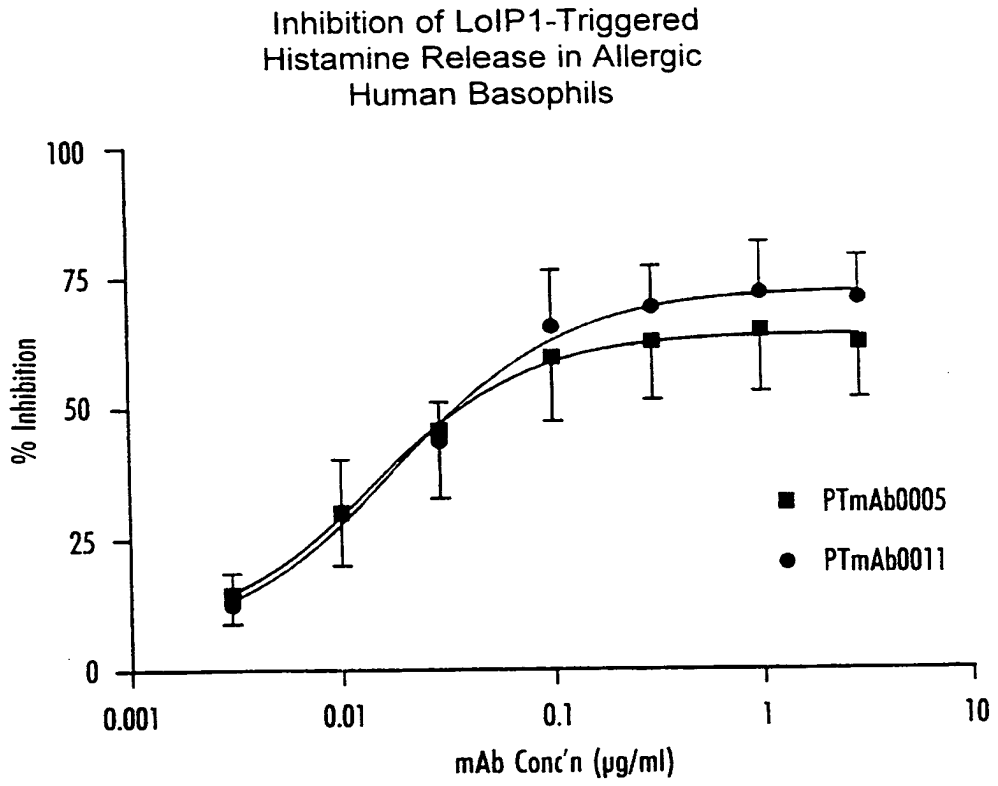
Inhibition of LoIP1-Triggered
Histamine Release in Allergic
Human Basophils
100
75
50
25
0
% Inhibition
0.001
0.01
0.1
1
10
mAb Conc'n (µg/ml)
PTmAb0005
PTmAb0011

Fig. 22 PTmAb0011 binding to different IgE.

A. Chimaeric IgE

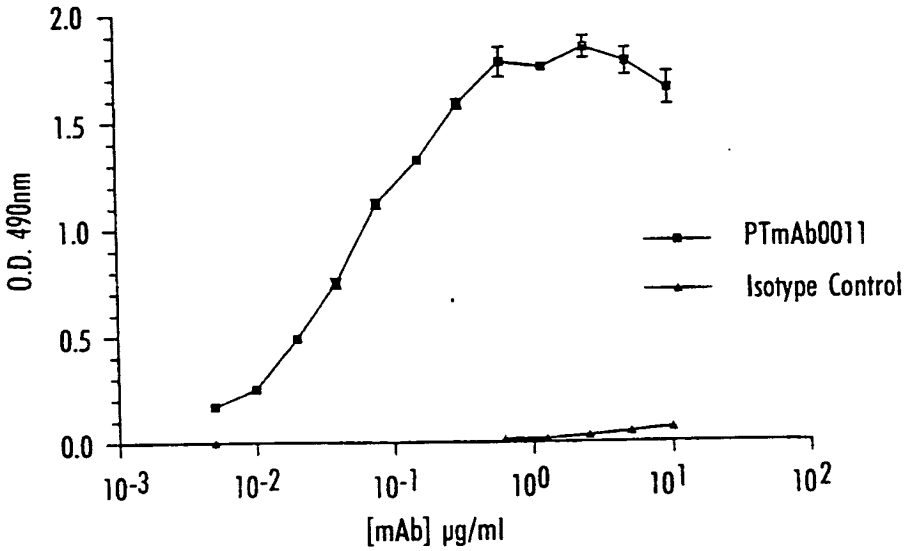

B. Binding to Myeloma IgE

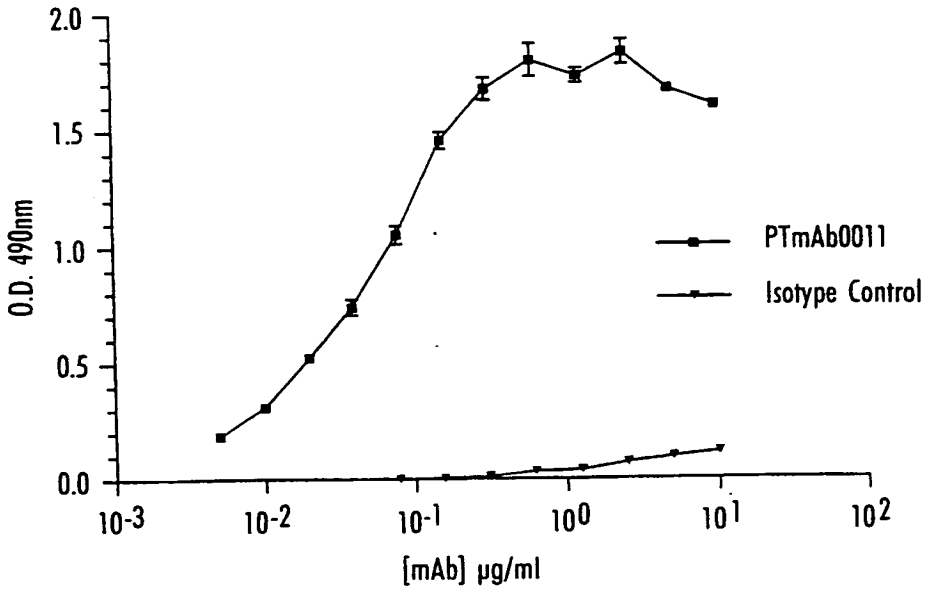

Fig. 22

C. Binding to Antigen Orientated IgE

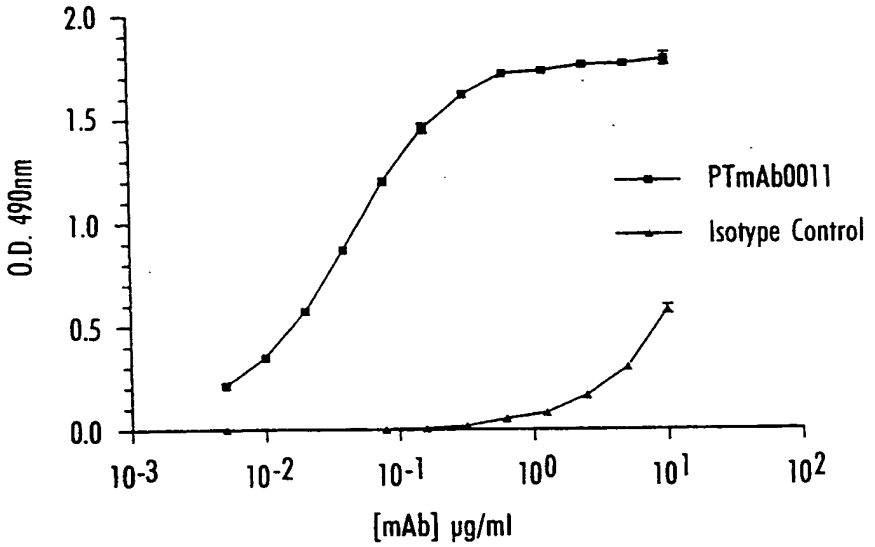

D. Binding to Heat Denatured IgE

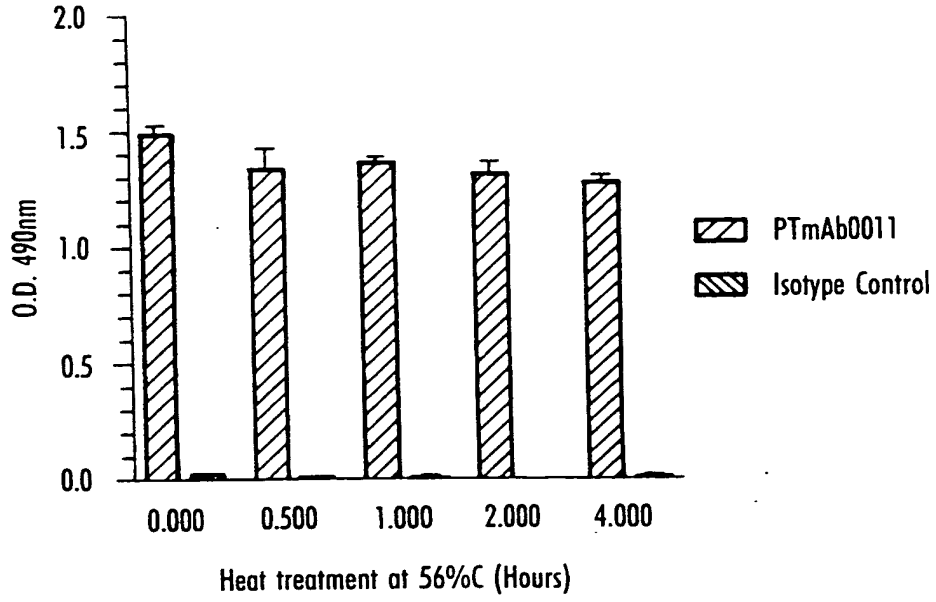

Fig. 23 Inhibition of IgE Binding to FcεR1α by PTmAb0011.

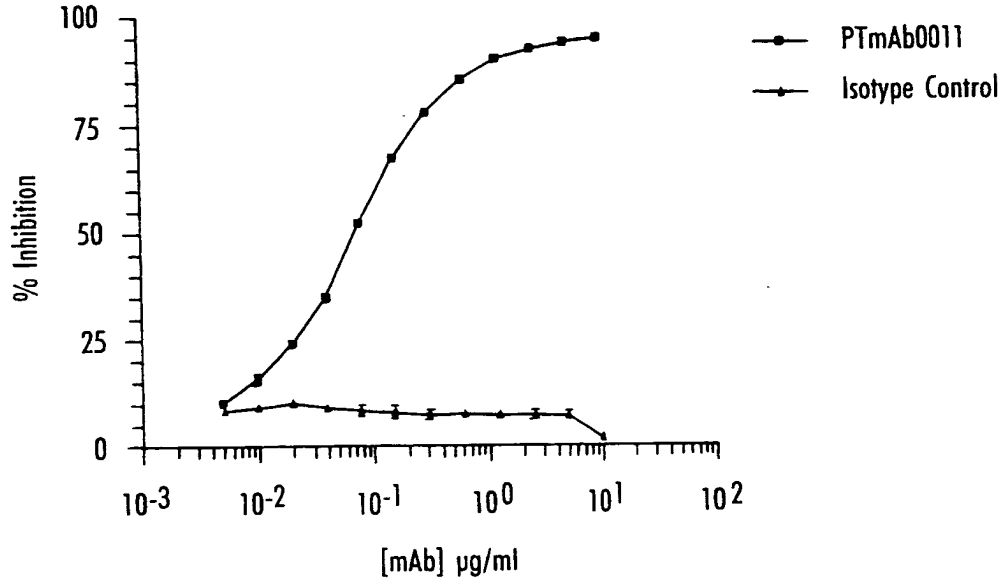

Fig. 24 Binding of PTmAb0011 to Receptor Bound IgE.

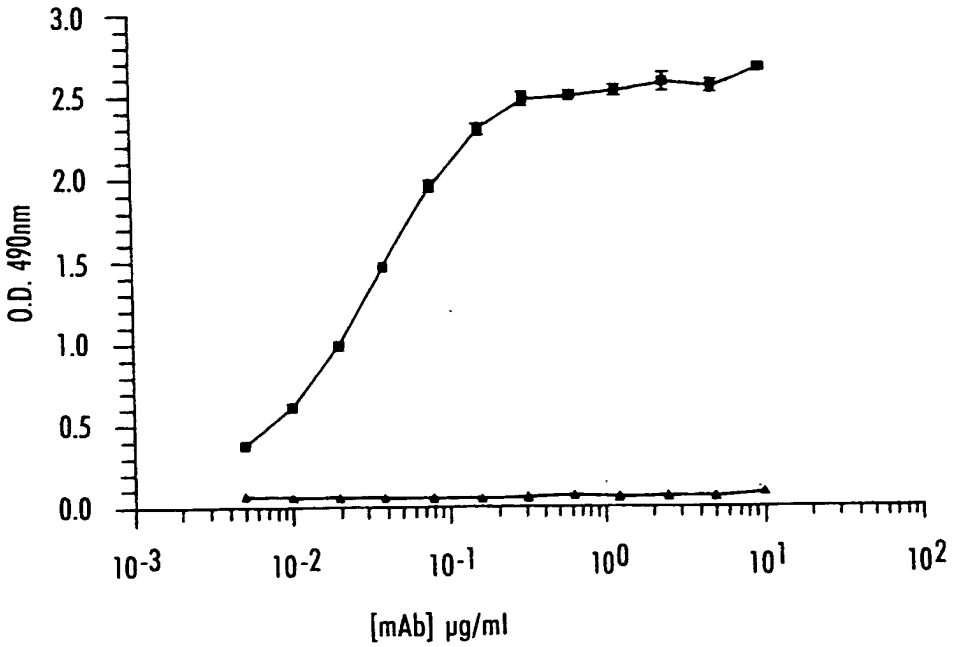

Fig. 25 The effect of PTmAb0011 on IgE binding to FcεRII on RPMI 8866 cells.

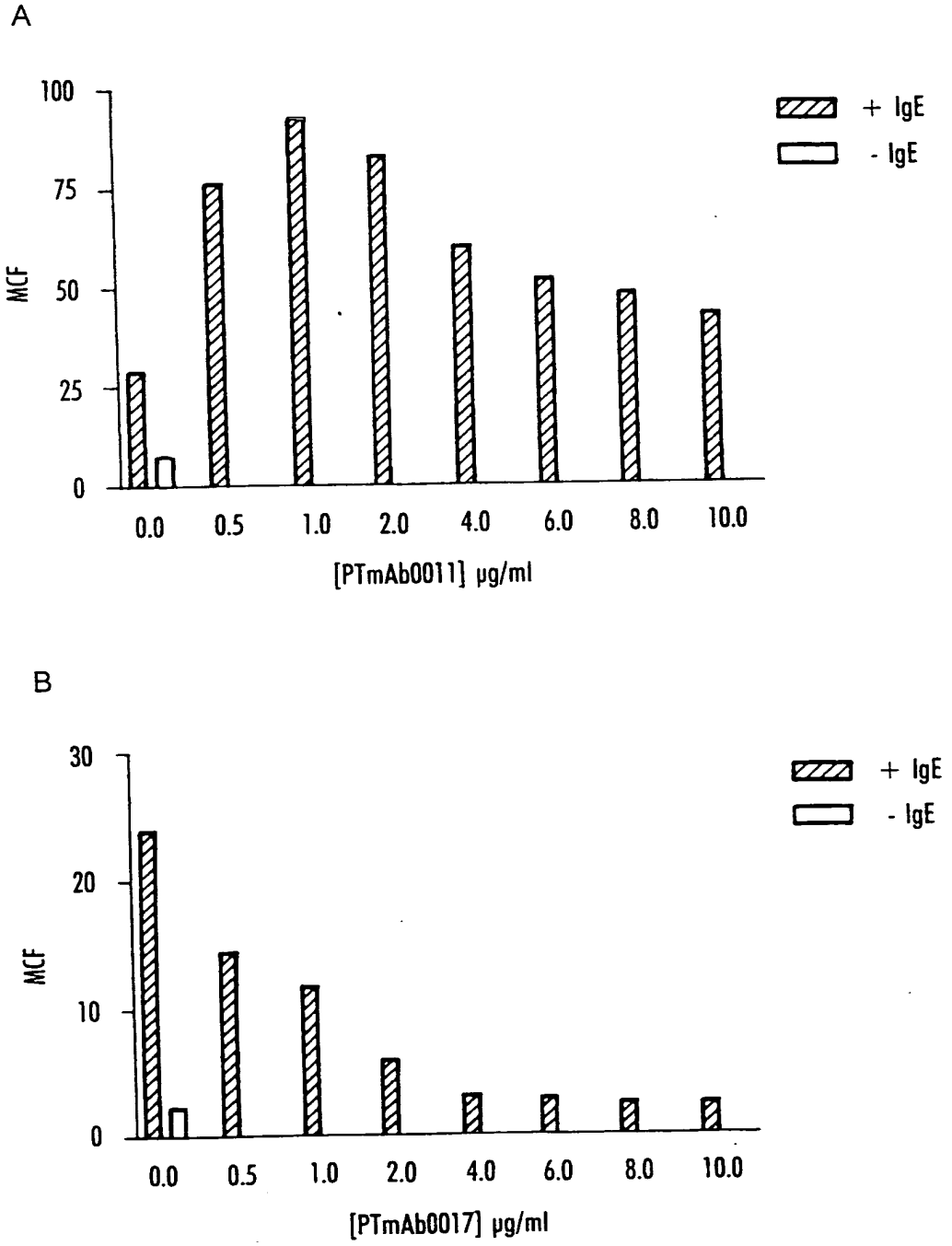

Fig. 26 Analysis of the effects of PTmAb0011 on IgE binding to FcεRII on primary human B-cells.

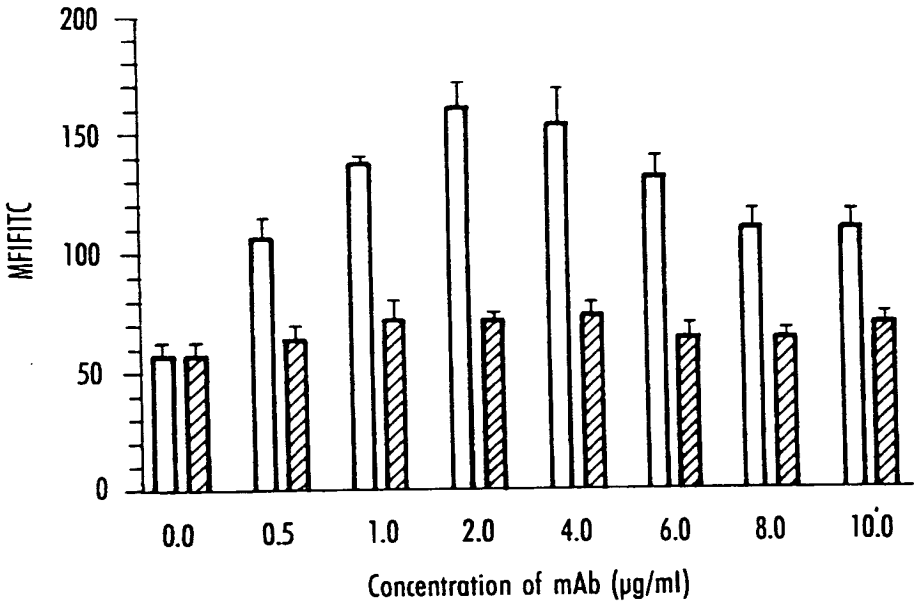

Fig. 27 Effects of PTmAb0011 on IgE secretion from primary human B-cells.

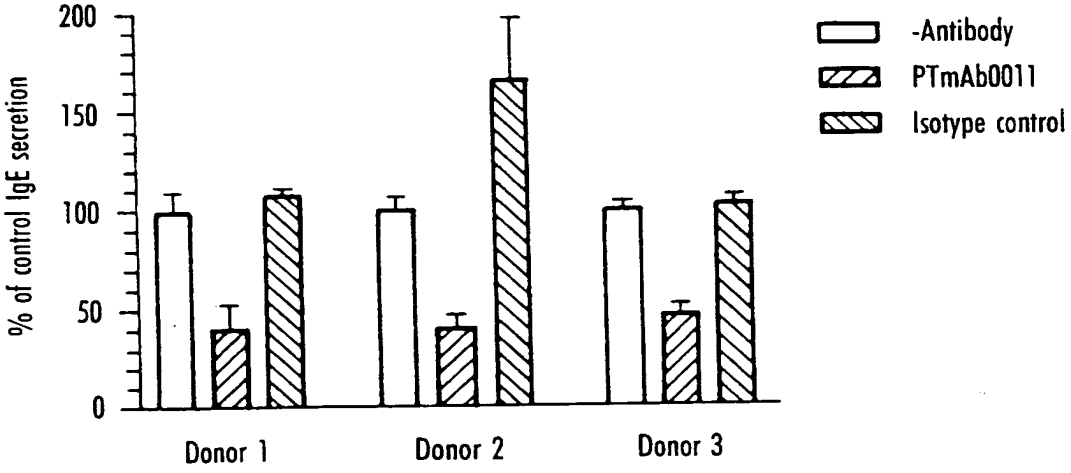

Fig. 28 Anaphylactogenicity of anti-human IgE monoclonal antibodies in allergic (A) and non-allergic (B) human basophils

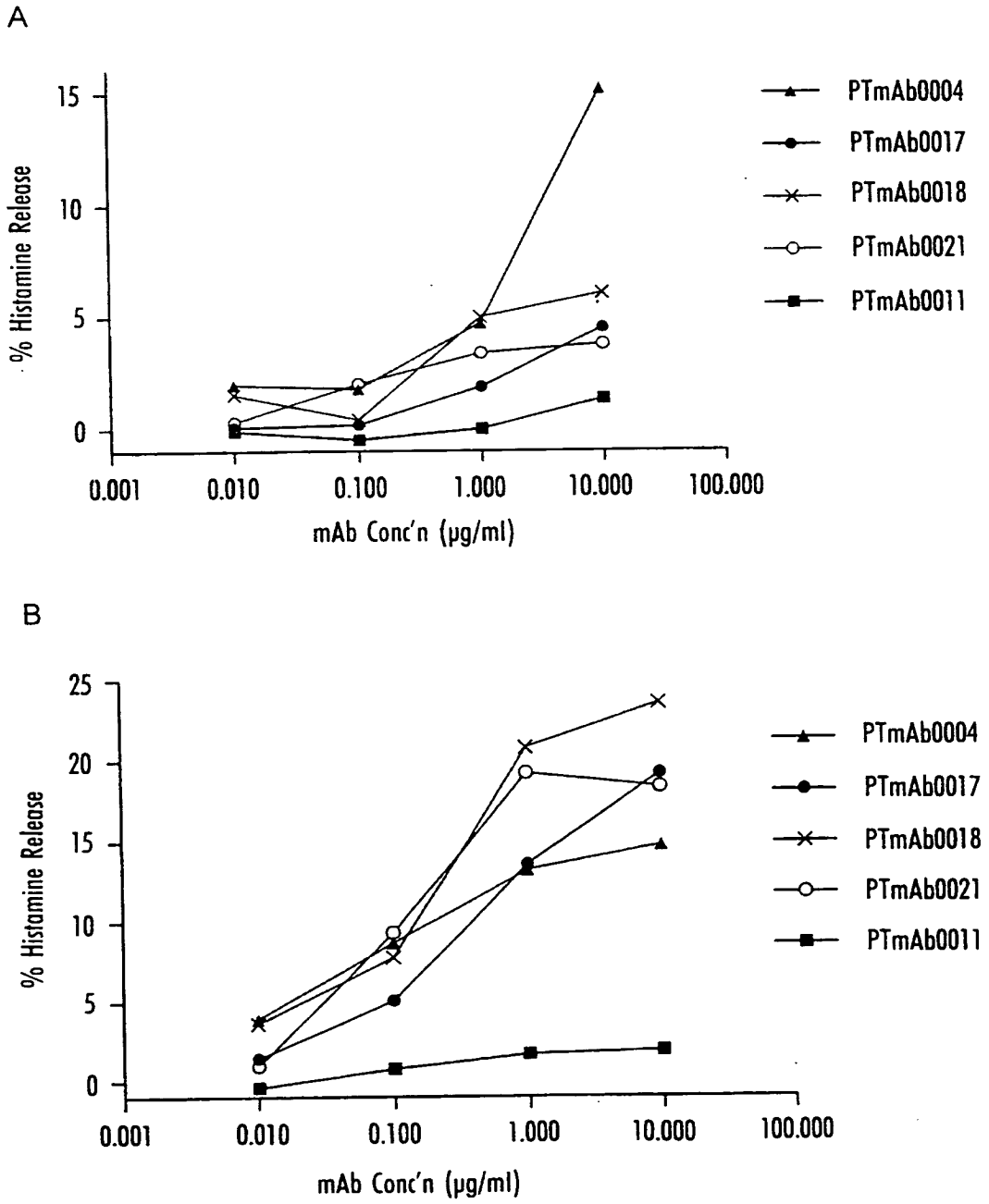

Fig. 29 Anaphylactogenicity of anti-human IgE antibodies in sensitised (A) and non-sensitised (B) human lung mast cells

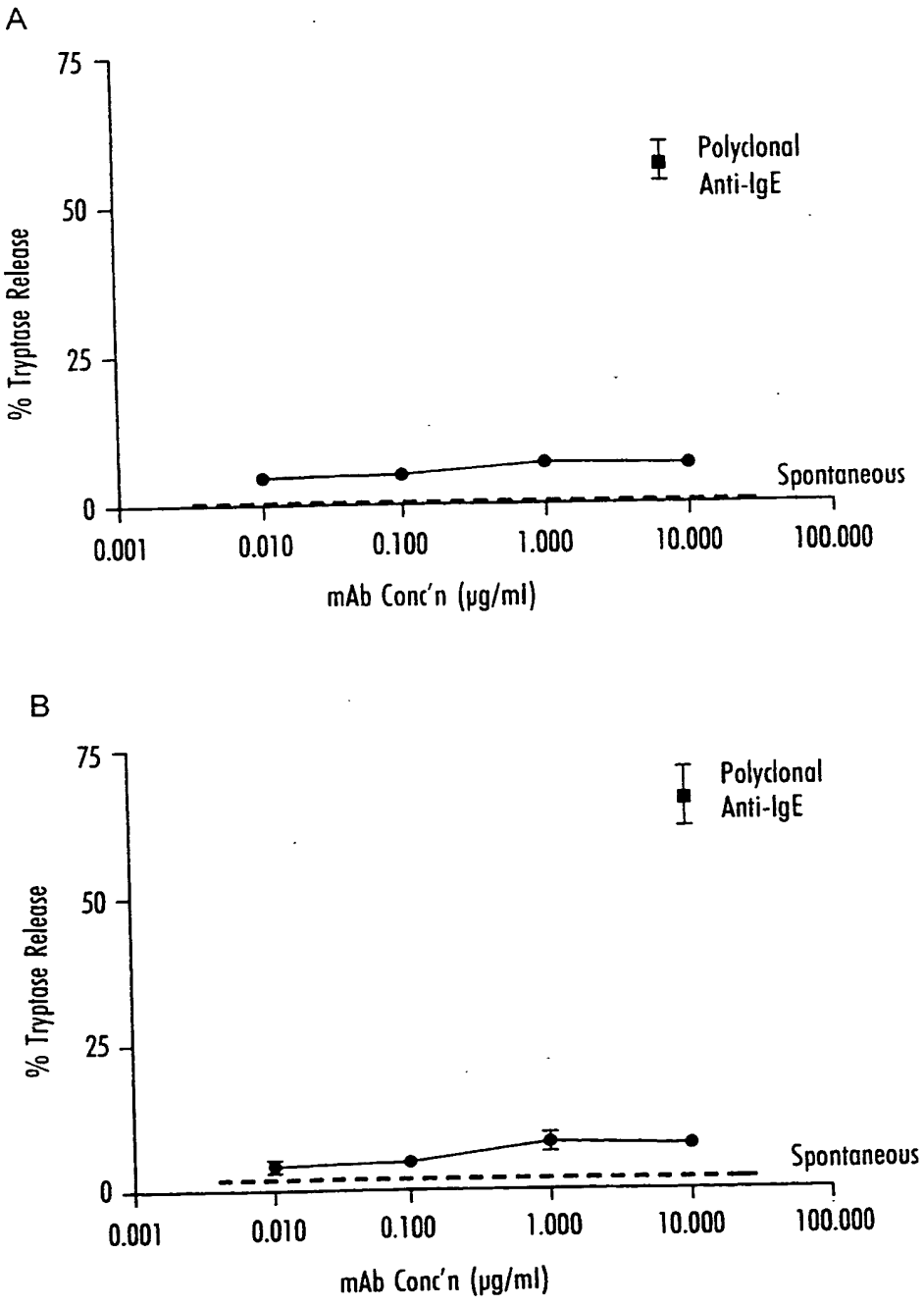

Fig. 30 Anaphylactogenicity of anti-human IgE antibodies in RBL J41 cells through human FcεRI (A) and mouse FcεRI (B)

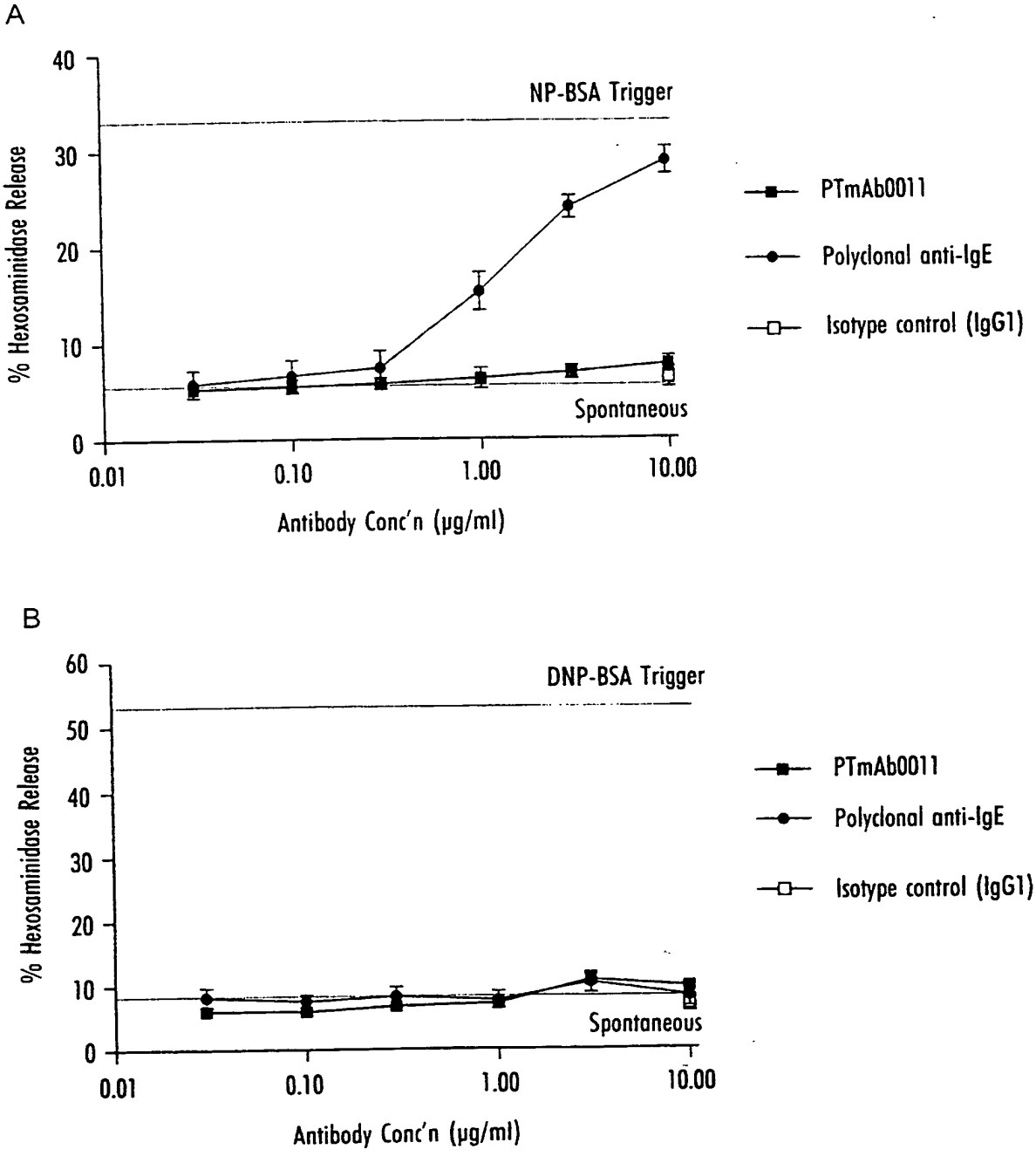

Fig. 31 Inhibition of allergen-triggered histamine release in human basophils by PTmAb0011

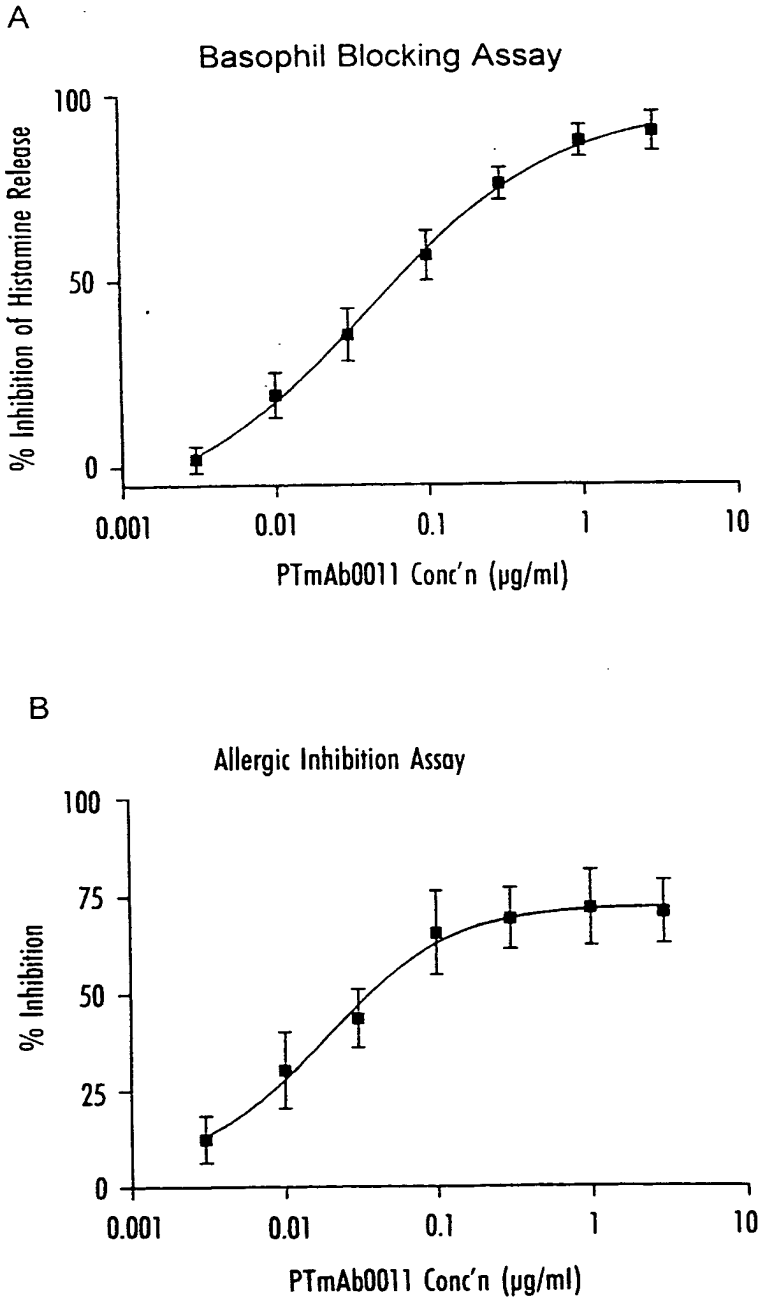

Fig. 32 Inhibition of passive cutaneous anaphylaxis in Monkey skin by PTmAb0011 and PTmAb0005.